NOTES AND CORRESPONDENCE

Conditional Probabilities of Significant Tornadoes from RUC-2 Forecasts

THOMAS M. HAMILL

National Center for Atmospheric Research, Boulder, Colorado*

ANDREW T. CHURCH

University of New Mexico, Albuquerque, New Mexico

29 September 1999 and 25 February 2000

ABSTRACT

Several previous studies have established statistical relationships between the severity of convection and environmental conditions determined from rawinsonde observations. Here, the authors seek 1) to determine whether similar relationships are observed when severe weather reports are associated with gridded *short-term numerical forecasts*, and 2) to develop and demonstrate a prototypal probabilistic model to forecast the likelihood a thunderstorm will be tornadic. Severe weather reports and lightning network data from 1 January 1999 through 30 June 1999 were used to classify the weather at a set of Rapid Update Cycle (RUC-2) grid points into four weather categories. These were no thunderstorms, nonsupercellular thunderstorms, supercellular thunderstorms without significant tornadoes, and thunderstorms with significant tornadoes (F2 or greater). RUC-2 forecast convective available potential energy (CAPE), helicity, and 0–4-km mean wind shear from the same period were associated with this gridded classification of the weather. In general similar relationships were found between environmental parameters and storm categorization as others have previously documented. The Bayesian probabilistic model used here forecasts the likelihood that a thunderstorm will produce a strong or violent tornado, given a certain value of CAPE and helicity (or CAPE and wind shear). For two selected cases when significant tornadoes occurred, this model reasonably located the high-threat areas many hours in advance of the severe weather. An enhanced version of this prototypal tool may be of use to operational severe weather forecasters.

1. Introduction

Forecasts of severe weather have improved substantially over the past few decades. Forecasters are using improved numerical weather prediction models and improved real-time data from sources such as Doppler radars, wind profilers, geostationary satellites, and the lightning detection network. As well, they now more thoroughly understand the dynamics of thunderstorms. Consequently, since 1973, the percentage of tornadoes occurring in a region within a tornado watch has increased from 30% to nearly 60% (McCarthy et al. 1998; Grice et al. 1999). Nonetheless, predicting severe thunderstorms other than by extrapolating the motion of existing severe storms is still quite difficult, and the interval where extrapolation is useful is quite short.

Many expect this trend toward more accurate tornado forecasts will continue as a result of improvements in numerical weather prediction models and assimilation schemes. Operational models continue to be upgraded and computed with smaller grid spacings (e.g., Rogers et al. 1996; Smirnova et al. 1997; Benjamin et al. 1998; Yucel et al. 1998). Within a few years we may have small enough grid spacings to *resolve* convective storms in our operational weather prediction model simulations. Despite this, chaos theory (Lorenz 1963, 1969) strongly suggests that it will always be difficult or impossible to *predict* the precise timing and location of these storms beyond a few hours (Islam et al. 1993), regardless of model resolution. Further, the smaller the scale of the phenomenon, then generally, the shorter the range of predictability. Given that precise numerical forecasts of severe weather are likely to remain problematic (Brooks et al. 1992), a realistic alternative goal is to relate the *probability* of mesoscale or microscale severe weather events to environmental conditions at the larger, more predictable scales.

Just what are the environmental parameters at larger scales that are related to severe weather and tornado

* The National Center for Atmospheric Research is sponsored by the National Science Foundation.

Corresponding author address: Dr. Thomas M. Hamill, NCAR/MMM/ASP, P.O. Box 3000, Boulder, CO 80307-3000.
E-mail: hamill@ucar.edu

potential? Miller (1972) and others have suggested the importance of buoyancy parameters; the most widely used now is convective available potential energy (CAPE; Moncrieff and Miller 1976). Chisholm and Renick (1972) and Fankhauser and Mohr (1977) discussed sounding characteristics typical of single-cell, multicell, and supercell thunderstorms, finding among other things that strong vertical wind shear was typical of supercells. Numerical simulations by Klemp and Wilhelmson (1978), Schlesinger (1980), Rotunno and Klemp (1982, 1985), Weisman and Klemp (1982, 1984, 1986), and Klemp (1987) examined the dependence of storm structure on wind shear and buoyancy through the use of a numerical cloud model. Using judiciously chosen thermodynamic and wind profiles, they demonstrated an ability to simulate storms that were qualitatively similar to those observed and to understand better the dynamics of storm-splitting and the deviate motion of supercells. Further, these latter findings suggest what environmental conditions are suitable for the development of particular types of severe storms (e.g., short-lived storms were associated with low shear and supercell storms associated with high shear).

Storm-relative helicity (SRH), which is related to streamwise vorticity, has also been suggested as an important predictor of supercells and/or tornadic activity (Lilly 1986; Davies-Jones 1984; Davies-Jones et al. 1990). Pictorially, helicity is proportional to the area swept out on a hodograph relative to the storm motion vector. Dynamically, helicity in the region of storm inflow indicates that vertical rotation will develop when horizontal shear is ingested into the storm and tilted into the updraft. Davies-Jones et al. (1990), Davies (1993), and Droegemeier et al. (1993) discussed the use of helicity as a forecast parameter for supercell thunderstorms. Recently, a number of authors have pointed out potential problems with using helicity, including a sensitivity to the estimated storm motion vector (Droegemeier et al. 1993; Weisman 1996; Weisman and Rotunno 2000) and the strong mesoscale variability that helicity can exhibit (Markowski et al. 1998b).

Several studies have attempted to establish statistical relationships between environmental conditions and severe weather. Davies and Johns (1993) discussed the relationship of wind shear and helicity to strong and violent tornadoes. Johns et al. (1993) similarly discussed the relationship between the severity of tornadoes and combinations of wind and buoyancy parameters. Brooks et al. (1994a) found useful information in column maximum specific humidity, helicity, and midtropospheric wind speed. Rasmussen and Blanchard (1998, hereafter RB98) developed statistical relationships between thunderstorm severity and environmental parameters. When convection occurred (as determined from lightning network data), the convection was classified as nonsupercellular, supercellular without signficant tornadoes, or supercellular producing significant tornadoes, depending on the severe weather report (since the classification was not performed with radar data, the authors acknowledged that there may have been significant errors in the assignment to these categories). RB98 determined the associated environmental parameters using a relatively nearby 0000 UTC sounding, presumably located in the inflow sector of the event. Parameters such as mean shear, helicity, CAPE, and combinations thereof were examined. Individual parameters were generally shown to discriminate less effectively between the three thunderstorm classifications than combinations of parameters such as CAPE and 0–4-km mean shear or CAPE and helicity.

RB98's study used observed sounding data. However, if tornado likelihood is to be forecast many hours prior to tornado occurrence, environmental conditions from numerical model forecasts will be required instead (e.g., Reap and Foster 1979; Stensrud et al. 1997). To this end, we have collected half a year's worth of Rapid Update Cycle (RUC-2) analyses and 12-h forecasts and severe weather observations. Our aims are 1) to determine whether some previously documented relationships between severe weather and environmental parameters are similar when these parameters are diagnosed from model analyses or 12-h forecasts rather than from rawinsonde data, and 2) to develop a probabilistic forecast model for the conditional probability of significant tornadoes (F2 or greater) using RUC-2 12-h forecast parameters. This probabilistic model will be based exclusively on combinations of CAPE and 0–4-km mean shear or CAPE and helicity. These parameters (and many others) are considered when the National Weather Service's Storm Prediction Center (SPC) generates their severe weather outlooks (Johns and Doswell 1992; Doswell et al. 1993).

The probabilistic model we will describe here should be considered a prototype, a simple, test version of an automated prediction algorithm that uses widely accepted measures of basic environmental conditions associated with severe weather. We acknowledge that there are many other potentially crucial factors relating to severe storm development, including the amount of convective inhibition, specific triggering mechanisms such as outflow boundaries or drylines (e.g., Markowski et al. 1998a; Rasmussen et al. 1999), and mechanisms for generating low-level mesocyclogenesis (Rotunno and Klemp 1985; Brooks et al. 1994b; Gilmore and Wicker 1998). We will not consider such additional effects here but acknowledge the wisdom of considering them in later studies, as well as the wisdom of collecting and analyzing many years' worth of data and revising the classification scheme.

The note is organized as follows. Section 2 describes the data and methodology. The method for categorizing storms as tornadic, supercellular, or nonsupercellular will be described, as well as our methods for calculating shear and helicity parameters. Section 3 compares the relationships between storm types and environmental conditions to those found in RB98. Section 4 then de-

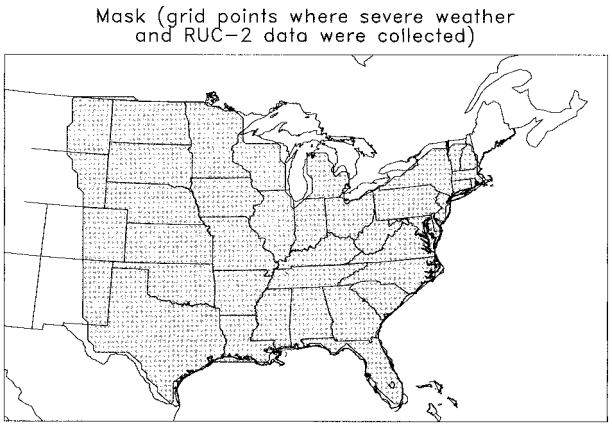

FIG. 1. Area where RUC-2 forecasts and the categorization of severe weather are associated in this study (shaded region).

scribes the probabilistic forecast model we developed. Section 5 presents some prototypal tornado probability forecasts using this model and discusses these forecasts. Section 6 concludes.

2. Data and methodology

a. Classification of observed weather at model grid points

In order to match severe weather events with gridded forecast data, we developed an algorithm to classify the observed weather at RUC-2 model grid points. Because of the paucity of reported data in the west, the developmental data was based only on a ''masked'' subset of points in the central and eastern United States (shaded points in Fig. 1). The severe reports analyzed here originated from the *Storm Data* final log of quality controlled severe reports from 1 January 1999 through 30 June 1999. The log provides the timing, location, and intensity of tornadoes, hail (and its size), and nontornadic damaging wind reports. Only reports from 2200 to 0200 UTC were used in this study; it was assumed that this time window could be associated reasonably with numerically forecast or analyzed conditions at 0000 UTC. Approximately half of the tornadoes in a 24-h period occurred within this 4-h window. The National Lightning Detection Network, operated by Geomet Data Services, Inc., provided the cloud-to-ground (CG) lightning strike data.

The composited severe report and lightning databases were used to classify the weather at each RUC-2 grid point within the masked area into one of four mutually exclusive and collectively exhaustive categories, roughly following the classification methodology outlined in RB98. The reader is referred to that article for a rationale of this classification. The categories were 1) no thunderstorm, 2) nonsupercellular thunderstorm, 3) supercellular thunderstorm without significant tornado, or 4) supercellular with significant tornado. The grid point

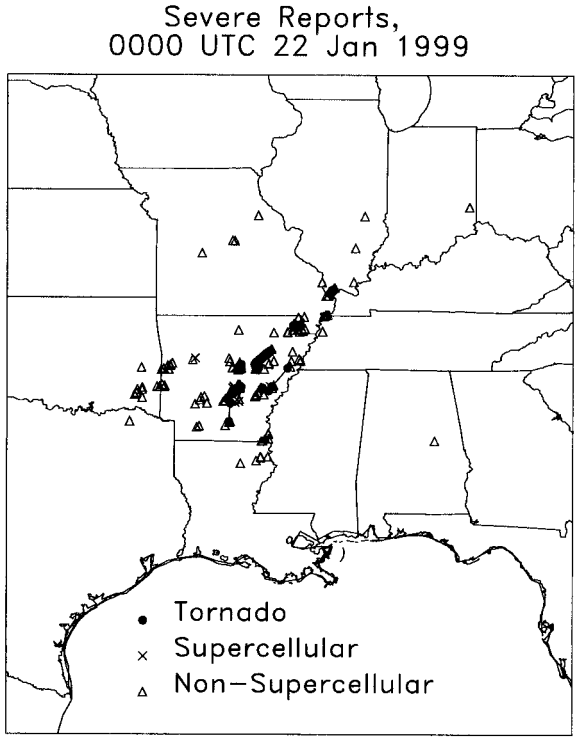

FIG. 2. Severe weather reports (using classification described in text) for the 4-h period centered on 0000 UTC 22 Jan 1999.

was classified as supercellular with significant tornado, or simply ''tornado'' if there was an observation of an F2 or greater tornado in that $(40\ \text{km})^2$ grid box during that interval. The grid point was classified as supercellular without significant tornado, or ''supercellular,'' if no F2 or greater tornado occurred within the grid box between 2200 and 0200 UTC, but hail of 2.0 in. (5.3 cm) or greater occurred. The grid point was classified as a nonsupercellular thunderstorm, or simply ''nonsupercellular,'' if more than two CG lightning strikes occurred in the grid box between 2200 and 0200 UTC and/or an F1 or F0 tornado, hail <5.3 cm, or damaging winds were reported. No thunderstorm took place in the grid box surrounding the grid point if no severe reports, no tornado reports, and two or fewer CG lightning strikes occurred (the choice of two is admittedly somewhat arbitrary). This scheme differs slightly from the RB98 scheme; we include smaller hail, damaging winds, and F0 and F1 tornadoes in the nonsupercellular thunderstorm category to ensure our classification was collectively exhaustive. Illustrations of the classification process are provided in Figs. 2 and 3.

As do RB98, we acknowledge this classification is far from perfect; for example, radar data should have been used to determine which storms were or were not supercells rather than inferring this from hail and tornado reports. Also, we have used only half a year's data here, excluding much summertime convection, so the

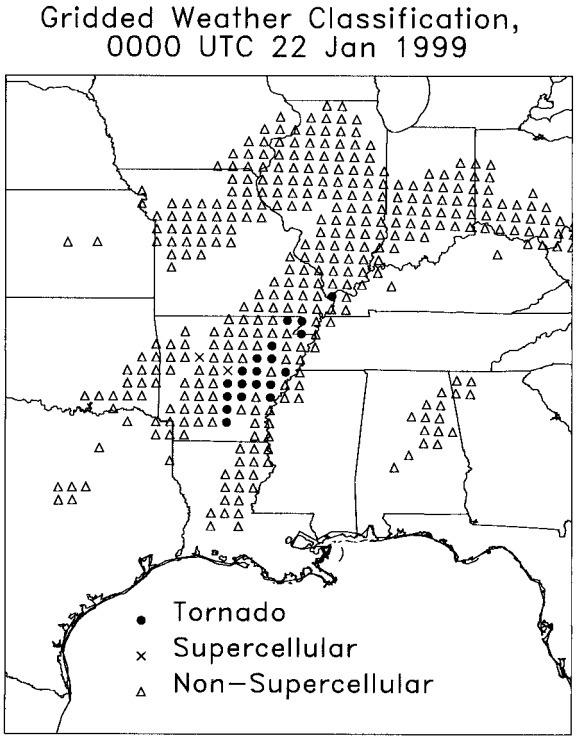

FIG. 3. Gridded analysis of thunderstorm type at RUC-2 grid points for the same 4-h period as in Fig. 2.

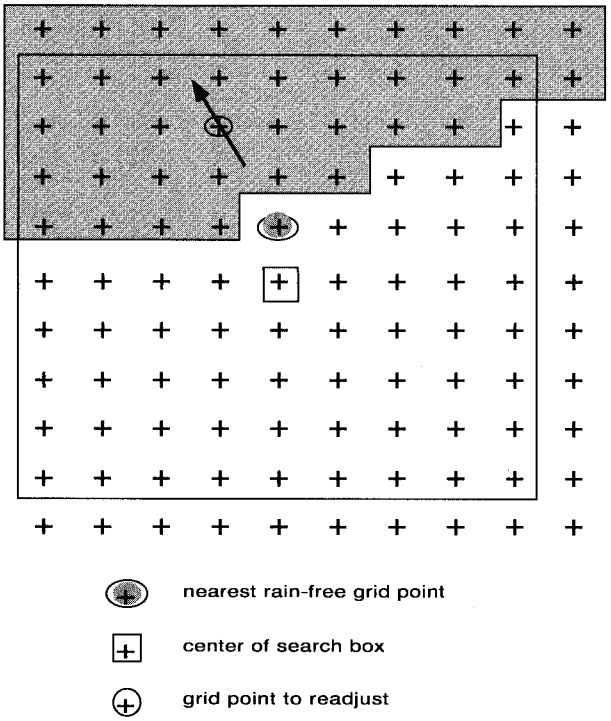

FIG. 4. Illustration of the method used for selecting an appropriate proxy grid point for a proximity sounding if it is raining at the original grid point. Shaded areas represent grid points where rain has accumulated during the past hour. Arrow indicates the direction of the surface wind. Boxed point denotes the center of search region. Solid line encompasses all grid points in search region. Filled circle indicates grid point selected as the nearest rain-free grid point upstream of the original grid point.

effects of small sample size should be also considered when interpreting our results.

Severe weather forecasters may find a different, more elaborate classification scheme more useful to their forecasting purposes. We chose to closely follow the RB98 classification here to permit us to compare results and because with our limited data, a refinement of the classification was not appropriate. Should we undertake subsequent work with larger datasets, we intend to revise the classification to make it more elaborate and useful to severe storm forecasters.

b. Defining CAPE, shear, and helicity from RUC-2 data

Environmental parameters were determined from the RUC-2 data as follows. RUC-2 0000 UTC analyses and 12-h forecasts from 1200 UTC conditions were used to define CAPE, wind shear, and helicity at model grid points inside the mask. Define

$$\text{CAPE} = g \int_{\text{LFC}}^{\text{EL}} \frac{\theta(z) - \overline{\theta}(z)}{\overline{\theta}(z)}\, dz, \qquad (1)$$

where LFC is the level of free convection, EL is the equilibrium level, $\theta(z)$ is the virtual potential temperature at height z of an air parcel ascending moist adiabatically from the LFC, $\overline{\theta}(z)$ is the virtual potential temperature of the environment, and g is the acceleration due to gravity. Prior to 6 May 1999, the air parcel was calculated from the parcel with the maximum 40-hPa average wet-bulb potential temperature in the lowest 180 hPa; after 6 May, this was extended to maximum in the lowest 300 hPa. Mean wind shear (Sh) refers to hodograph length between 0 and 4 km above ground level (AGL). We shall hereafter refer to this as the 0–4-km mean shear, or simply shear. Note that unlike the definition of this in RB98, we do not divide by the vertical depth of the shear layer. Helicity is calculated using 0–3 km AGL winds and following the Galilean-invariant methodology for calculating the storm motion vector described in Bunkers et al. (2000). Helicity (SRH) is defined here as

$$\text{SRH} = -\int_{0}^{3\text{ km}} \mathbf{k} \cdot (\mathbf{V} - \mathbf{c}) \times \frac{\partial \mathbf{V}(z)}{\partial z}\, dz, \qquad (2)$$

where $\mathbf{k}$ is the vertical unit vector, $\mathbf{c}$ is the storm motion vector, and $\mathbf{V}(z)$ is the horizontal velocity vector.

If model-generated convection is occurring at a forecast grid point at 0000 UTC, its forecast sounding may be unrepresentative of the preconvective environmental condition. In this case, the forecast sounding at that grid point is considered to be ''contaminated'' by model convection, and another sounding point may need to be

chosen. To address this, we have developed our own proximity sounding method, as illustrated in Fig. 4. If there is rain occurring at a model grid point, a set of adjacent grid points is examined to determine if any of them are rain free. This set of adjacent grid points is determined by first finding the grid point that is 160 km upstream of the rainy grid point, with the upstream direction defined using model-forecast surface winds. A 9×9 array of grid points centered on this upstream grid point is considered, and the nearest rain-free grid point to the original rainy grid point is located. If the CAPE at this rain-free grid point is greater than the CAPE at the rainy grid point, then the CAPE, shear, and helicity values from the rain-free grid point replace the values at the rainy point. If the rainy point's CAPE value is higher or if all boxes in the 9×9 array were rainy, this point retains its original CAPE, shear, and helicity. If we had RUC-2 data available at very high temporal resolution, then ideally we would simply use the RUC-2 conditions at the grid point for the forecast hour immediately preceding the onset of convection. However, since we lacked this high temporal resolution data, this approximate algorithm was chosen to address some of the issues of rain-contaminated model forecast soundings.

3. Relationships between weather and environmental parameters

Here, we analyze the relationship between the classified weather and the environmental parameters using statistics similar to those used in RB98. This permits ready comparison to see if the relationships are robust despite our use of model-analyzed and forecast data (as opposed to RB98's use of raob's), and given our slightly different analysis methods. We will examine the relationships between the weather classification and CAPE, helicity, 0–4-km mean shear, the energy–helicity index (Hart and Korotky 1991; Davies 1993), and the so-called vorticity generation parameter (VGP; RB98). The energy–helicity index (EHI) is defined as

$$\text{EHI} = \frac{\text{CAPE} \cdot \text{SRH}}{1.6 \times 10^5}. \tag{3}$$

Previously, EHI > 2.0 was suggested as indicating a larger probability of supercells (RB98). The VGP parameterizes the rate of conversion of horizontal to vertical vorticity through tilting. It is defined as

$$\text{VGP} = \frac{\text{Sh}\sqrt{\text{CAPE}}}{4000\ \text{m}}. \tag{4}$$

Consider first the scatterplots of weather as a function of RUC-2 12-h forecast CAPE and shear (Figs. 5a–d) and CAPE and helicity (Figs. 6a–d). There are drastically many more points with no thunderstorms or nonsupercellular thunderstorms than with tornadic or supercellular thunderstorms, emphasizing the rarity of these events. However, the ratio of the frequency of tornadoes relative to nonsupercellular thunderstorms is much larger at higher CAPE and shear values than it is at lower CAPE and shear values. That is, at lower CAPE and shear, ordinary thunderstorm counts overwhelm tornado counts, but at higher CAPE and shear, the relative proportions of tornadic, supercellular, and nonsupercellular thunderstorms are much more similar.

These relationships can be better visualized with box and whisker plots, as in RB98. For CAPE (Fig. 7), notice the RUC-2 data distributions have higher CAPEs relative to RB98 values, perhaps because of RUC-2 model bias or a difference in the method of calculating the wet-bulb potential temperature of the parcel (section 2b). Also, recall that our definition of nonsupercellular convection is slightly different from the definition used in RB98; we include F0 and F1 tornadoes and reports of hail <5.3 cm; they do not. This may tend to bias our nonsupercellular CAPE, shear, and helicity values toward slightly higher values than in RB98. Despite this, the ability to discriminate between the three thunderstorm types from RUC-2 CAPE is quite similar to the ability demonstrated with sounding data in RB98.

Box and whisker plots for 0–4-km mean shear are shown in Fig. 8. The ability of shear to discriminate between thunderstorm types is somewhat different for the analysis and forecast data. For example, notice that for supercells, the mean shear changes from 27.8 m s^{-1} in the RUC-2 analysis to 20.2 m s^{-1} in the forecast. Whether this is a result of the relatively small sample size owing to using 6 months of data or due to RUC-2 model biases or smoothing effects is unclear. However, as in RB98, significant tornadic thunderstorms generally are associated with higher shears. Also there does appear to be a shear threshold for tornadoes more noticeable than that found in RB98; here, 90% of the significant tornadoes occurred when shear was $\sim$25 m s^{-1} or greater. No such threshold at a relatively high shear existed for the nonsupercellular thunderstorms. This result is generally consistent with previous modeling studies (e.g., Weisman and Klemp 1986) and observational studies (e.g., Davies and Johns 1993).

Helicity (Fig. 9) appears to discriminate rather well between tornadic thunderstorms and the other two classifications, better than in RB98. There also appears to be a lower limit to helicity below which significant tornadoes are extremely unlikely (e.g., Davies-Jones et al. 1990; Stensrud et al. 1997). Note that our classification methodology uses a different, presumably improved method for calculating storm motion (Bunkers et al. 2000) than was used in RB98.

As in RB98, we examined combinations of parameters, namely, the EHI (Fig. 10) and VGP (Fig. 11). As with RB98, the EHI discriminated relatively well between the three storm severities. EHI values were generally higher than in RB98 because the input CAPE values were larger, but there is a similar ability to discriminate among the three storm types. The VGP is

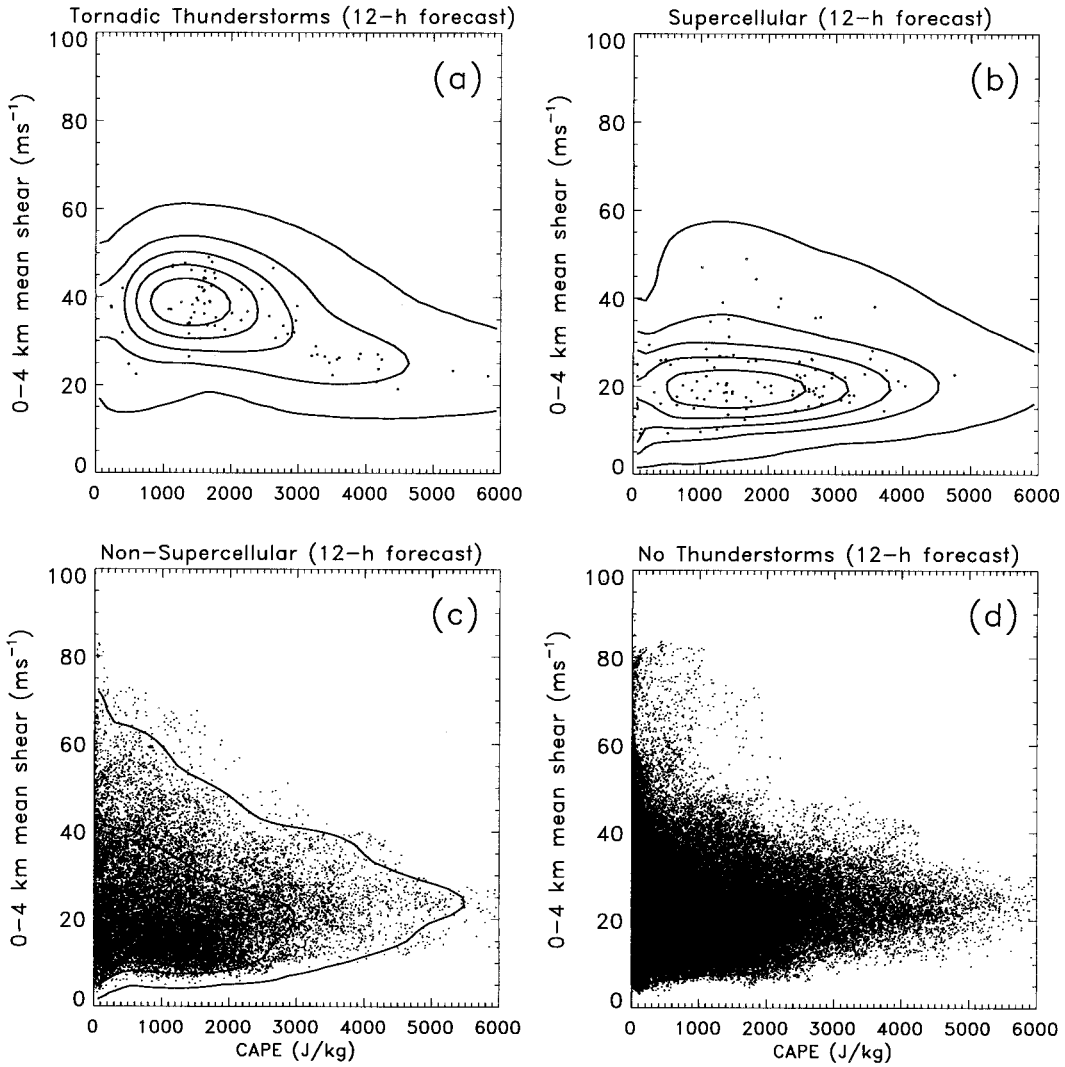

FIG. 5. Scatterplots of weather types as a function of CAPE and 0–4-km 12-h forecast mean wind shear from the RUC-2 model. Contours of fitted probability density functions are overplotted (10th, 30th, 50th, 70th, and 90th percentiles). (a) Tornadic thunderstorm, (b) supercellular thunderstorm, (c) nonsupercellular thunderstorm, and (d) no thunderstorm.

slightly less effective as a discriminator than the EHI, but this is qualitatively consistent with the results in RB98.

Overall, the relationships demonstrated in this section suggest that RUC-2 forecast data do have enough ability to discriminate between nonsupercellular, supercellular, and tornadic storms to suggest the potential usefulness of these data in a probabilistic model.

4. Model for conditional probabilities of significant tornadoes

We now turn our attention to how RUC-2 forecast CAPE and shear (or helicity) information can be used to model the likelihood of significant tornado occurrence, given that a thunderstorm occurs. Such a model could be used as a forecast tool to quickly determine areas with an enhanced risk of tornadoes. Note that we will demonstrate only a model for the conditional probability a thunderstorm being tornadic, but no model of unconditional probabilities or the probability of thunderstorms. We believe the development of these models would be useful, though in developing them it may be especially important to consider other potentially important parameters such as convective inhibition and the effects of low-level boundaries as triggering mechanisms (Markowski et al. 1998a; Rasmussen et al. 2000).

How might conditional tornado probabilities be forecast using the CAPE and shear information in Fig. 5? Given a RUC-2 forecast of CAPE and shear, a crude

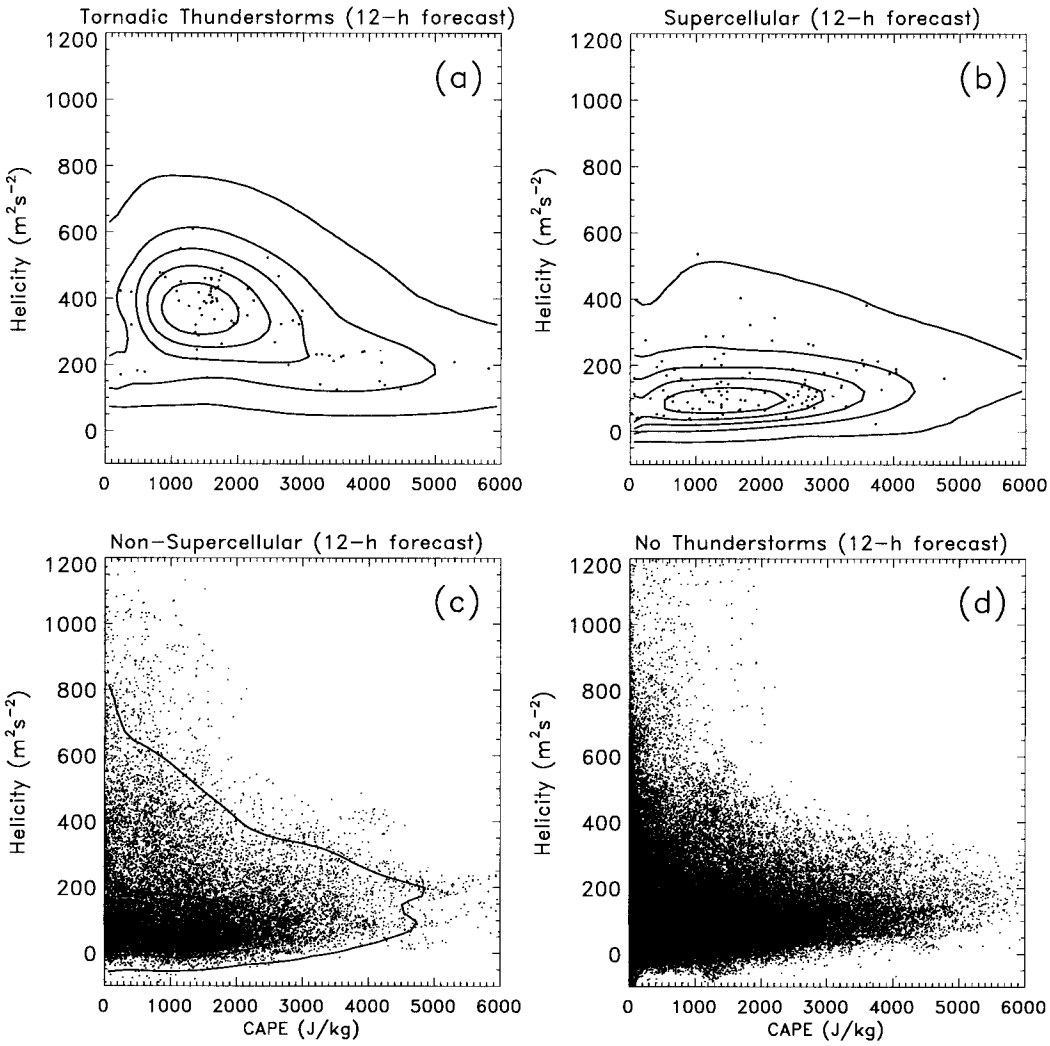

FIG. 6. As in Fig. 5 but for CAPE vs helicity.

estimate could be made of the conditional probability of tornadoes; the number of dots around particular CAPE and shear values in Fig. 5a could be counted and divided by the total number of dots around that CAPE and shear in Figs. 5a–c. However, notice that the dots tend to be clustered, so some of the variation in the density of dots is probably unrealistic. This is because our dataset has a small sample size and because parameters values among the samples are correlated (i.e., a cluster of dots may reflect a tornado outbreak with data points with similar CAPE and shear values). Hence, some way of ''smoothing'' the gradations of dots would be helpful.

The starting point for an improved model is Bayes' rule (Wilks 1995). In this model, let B be the compound event that CAPE and shear Sh have certain forecast values. For example, B might be the event that Sh $\cong$ 20 m s^{-1} and CAPE $\cong$ 3000 J kg^{-1}. Let T be the event that a RUC-2 grid box is classified as tornadic; let S be the event that it is classified as supercellular; and let R be the event that it is classified as a nonsupercellular thunderstorm. Then, Bayes' rule states

$$P(T|B) = \frac{f(B|T)P(T)}{f(B)}, \tag{5}$$

where

$$f(B) = \sum f(B|T)P(T) + f(B|S)P(S) + f(B|R)P(R). \tag{6}$$

Here, $P(T) = n_T/(n_T + n_S + n_R)$, $P(S) = n_S/(n_T + n_S + n_R)$, and $P(R) = n_R/(n_T + n_S + n_R)$, where n_T, n_S, and n_R indicate the total number of grid boxes classified as either tornadoes, supercellular, or nonsupercellular thunderstorms. That is, n_T, n_S, and n_R are the total number of dots in Figs. 5a–c, respectively. The probability density functions $f(B|T)$ $\{= f[(\text{CAPE, Sh})|T]\}$, $f(B|S)$, and $f(B|R)$ represent the probability density of

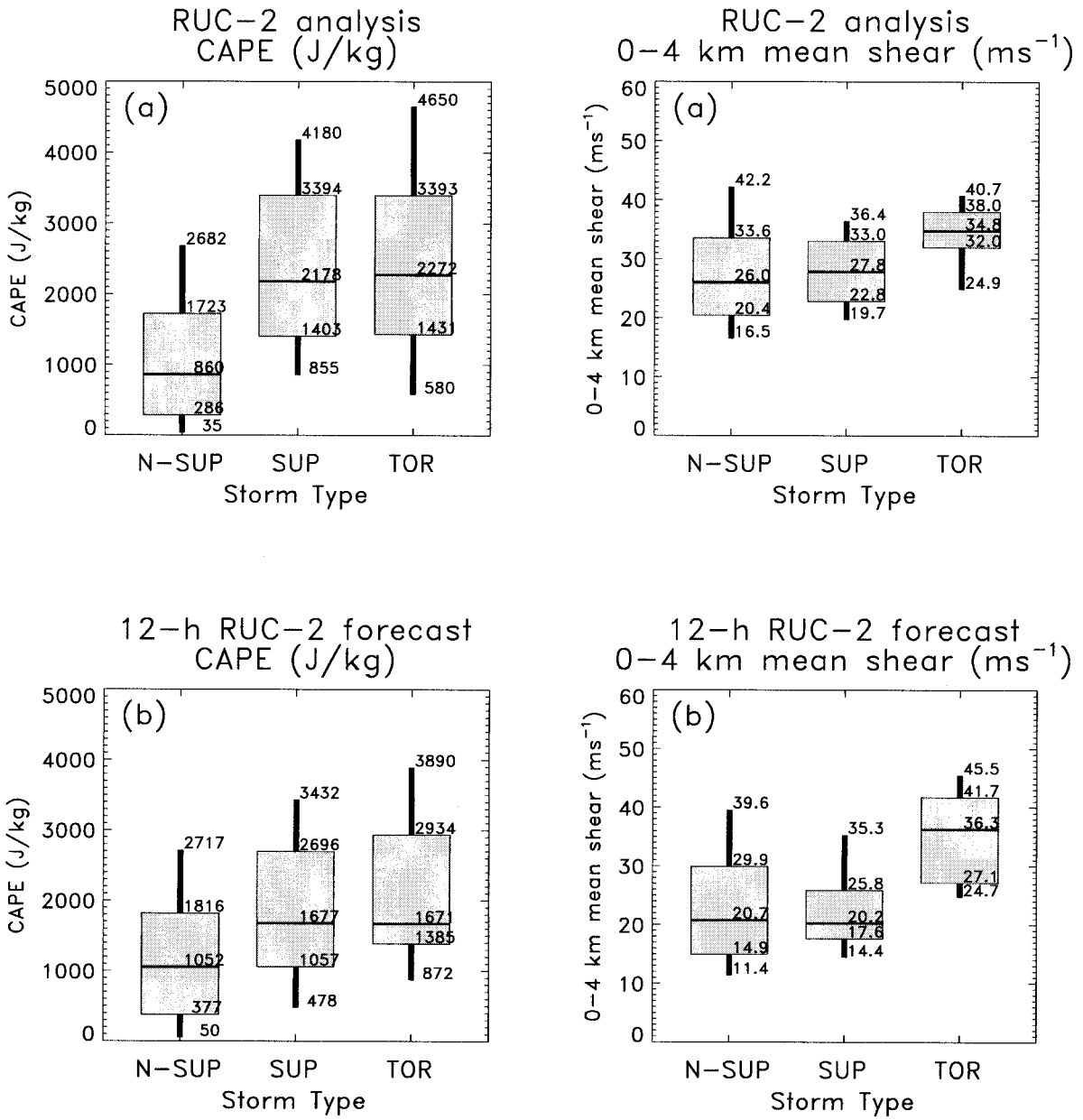

FIG. 7. Box and whisker plots for CAPE for the three storm types. Box top, middle, and bottom indicate the 75th, 50th, and 25th percentiles of the empirical distributions, and the top and bottom ends of the whisker denote the 90th and 10th percentiles, respectively. (a) RUC-2 analysis data, and (b) 12-h RUC-2 forecast data.

FIG. 8. As in Fig. 7 but for 0–4-km mean wind shear.

a particular CAPE and shear value, given that a tornadic, supercellular, or nonsupercellular thunderstorm occurs, respectively. Qualitatively, they are related to the local density of dots on each of the diagrams relative to the density in other areas of the diagram.

We thus required an estimate of the probability density function for tornadoes as a function of CAPE and shear (and estimates for supercellular and nonsupercellular thunderstorms as well). We constrained the possible values of CAPE and shear to realistic maximum and minimum values and estimate densities within these parameter ranges. Specifically, $0 \leq \text{CAPE} < 6000$ J kg^{-1} and $0 \leq \text{Sh} < 100$ m s^{-1}. Probability density was required to integrate to 1.0 over this domain. The range of parameter values for $f(B|S)$ and $f(B|R)$ were similarly constrained. We assigned zero conditional probability of tornadoes if CAPE $= 0$.

We tried to estimate $f(B|T)$, $f(B|S)$, and $f(B|R)$ using parameteric probability density distributions such as the bivariate gamma distribution or bivariate normal distributions fitted to power-transformed data (Wilks

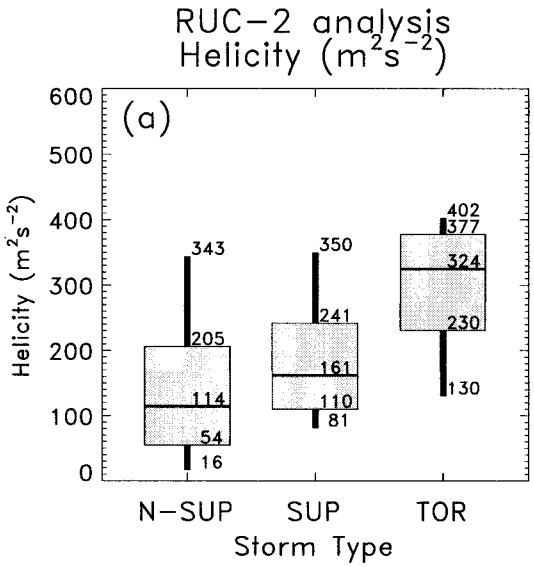

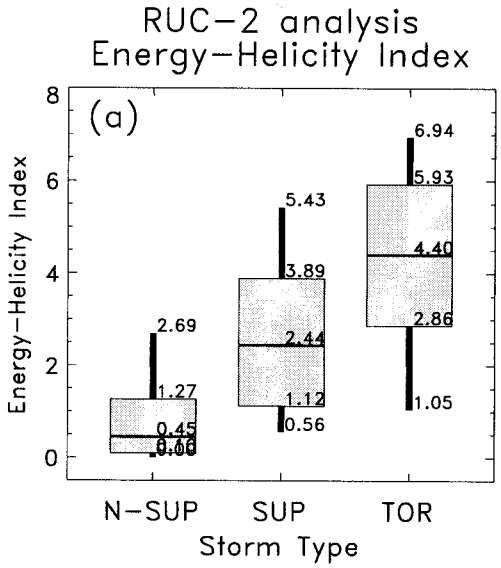

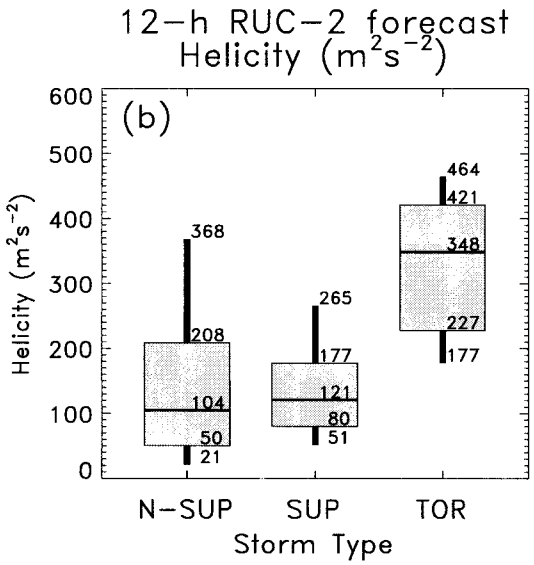

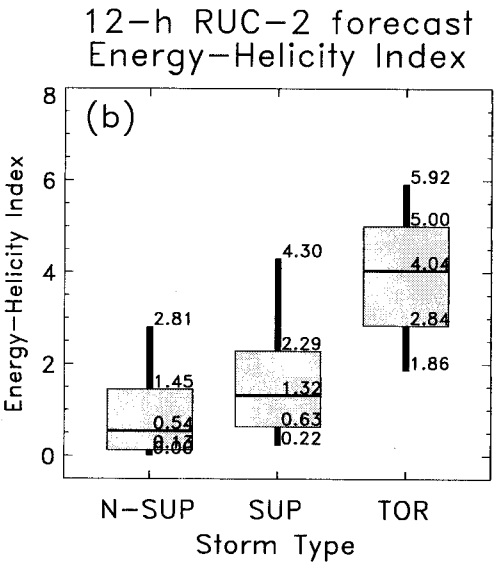

FIG. 9. As in Fig. 7 but for helicity.

FIG. 10. As in Fig. 7 but for the energy–helicity index.

1995). However, these methods produced unsatisfactory fits (not shown). Hence, we resorted to estimating $f(B|T)$, $f(B|S)$, and $f(B|R)$ using nonparametric density estimation techniques (Silverman 1986). The reader is referred to this very readable text for details on the application of this technique.

For our purposes, some unconventional extensions to standard nonparametric kernel techniques were required to produce reasonable density estimates. For example, we found that a transformation of coordinate systems to make the data more normally distributed was necessary before generating density estimates; application of the kernel technique when the data were strongly nonnormal resulted in erroneously low density estimates near zero CAPE. After density estimates were produced in the transformed coordinate system, the density estimates were transformed back to provide an estimate in the original, untransformed coordinate system.

We also found that larger window widths than one might expect were required to generate appropriately smooth density estimates, especially for the tornadic and supercellular categories. When conventional methods for estimating optimal window widths were used, such as cross validation, the resulting density estimates were

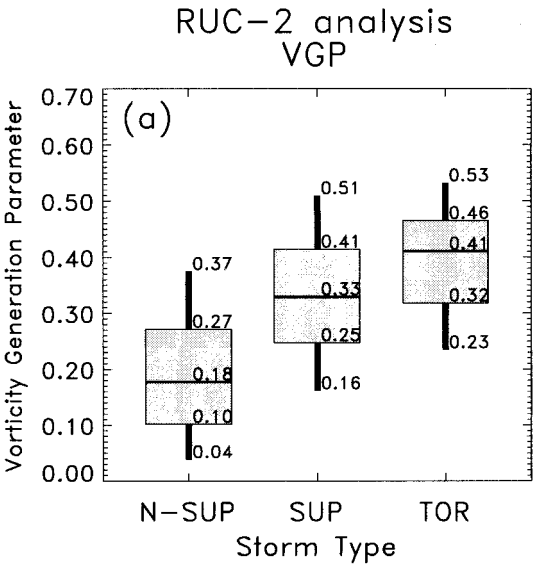

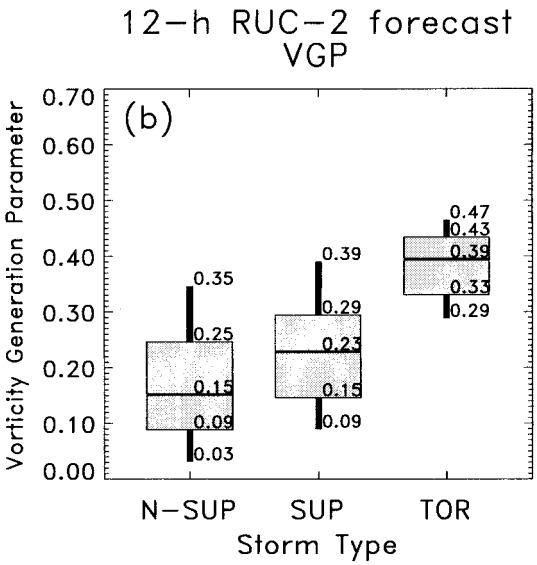

FIG. 11. As in Fig 7 but for the vorticity generation parameter.

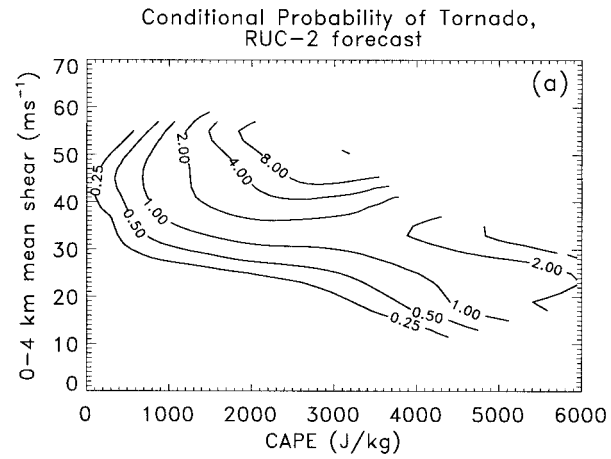

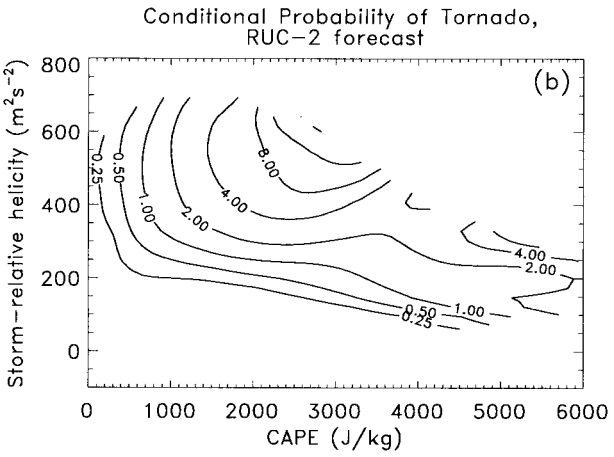

FIG. 12. Conditional probabilities of the occurrence of a tornado (in %) given that a thunderstorm occurs as a function of RUC-2 12-h forecast parameters (a) CAPE and 0–4-km mean shear, and (b) CAPE and helicity. Areas without contours were not sufficiently populated with samples to attempt a probability estimate or had negligibly small probabilities.

unrealistically ''lumpy.'' As mentioned previously, this was because individual observations could not be assumed to be independent, since severe weather reports typically occurred in clusters with similar CAPE–shear–helicity values. Hence, we subjectively selected what we believed were optimal window widths.

Contours of the probability density estimates are overlaid on the scatterplots in Figs. 5a–d and 6a–d. These probability density estimates are then used in conjunction with RUC-2 forecast parameters using (5) and (6) to determine the conditional probability a thunderstorm will be tornadic. An illustration of this model's estimate of conditional tornado probability as a general function of CAPE and shear and CAPE and helicity are shown in Figs. 12a,b. As expected, the probability of a tornado occurring generally increases with increasing CAPE and shear. Even with the relatively strong smoothing used to generate the density estimates, the probabilities have multiple maxima that are likely unrealistic. We expect that if we collected a longer sample of data, the incidence of tornadoes would not be concentrated specifically near one value of CAPE and helicity or shear, and these curves would become smoother and may not exhibit such multiple maxima.

Note that this model is designed similarly to Model Output Statistics (MOS; Carter et al. 1989); forecast equations are developed by relating observational data

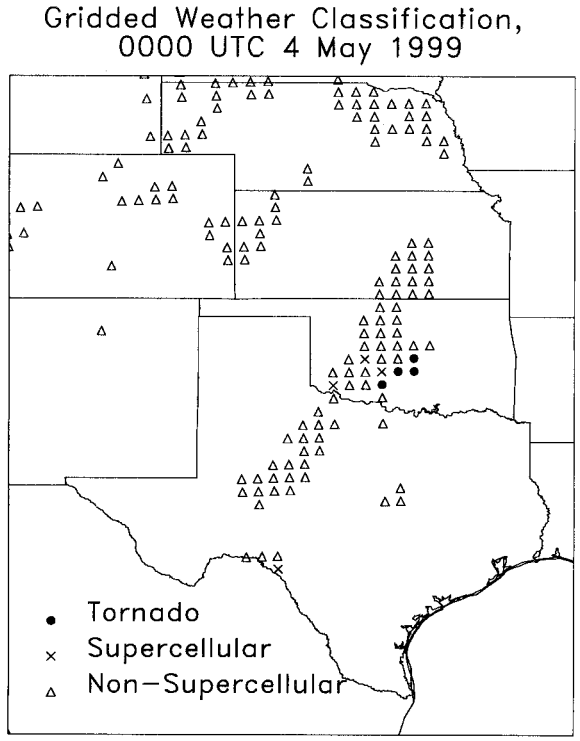

FIG. 13. As in Fig. 3 but for the 4-h period centered on 0000 UTC 4 May 1999.

to forecast model output. Hence, it has many of the same strengths and drawbacks of MOS. Most notably, if the model physics are stable, then this scheme can account for model biases. However, if model physics are changed, and new forecasts have substantially different biases than the old forecasts used as developmental data, then the accuracy and reliability of probability estimates will be degraded. Also, as with MOS, this approach cannot be expected to correct for random errors in position or magnitude of input fields. For example, if the axis of maximum CAPE is misforecast by the RUC-2, the axis of maximum tornado probability can be expected to be misforecast as well.

5. Results from probabilities model

We now provide some simple illustrations of conditional tornado probability forecasts generated from this model. We shall examine tornado forecasts valid at 0000 UTC on two days: 22 January 1999 and 4 May 1999. These dates are days with significant tornado outbreaks in Arkansas (Fig. 3) and Oklahoma (Fig. 13).

It is important to develop the probabilistic model with a different dataset than is used to evaluate it. To this end, when producing forecasts for 22 January 1999, for example, this day's data points were excluded from the dataset used to develop probability estimates, with similar exclusion when producing 4 May 1999 forecasts.

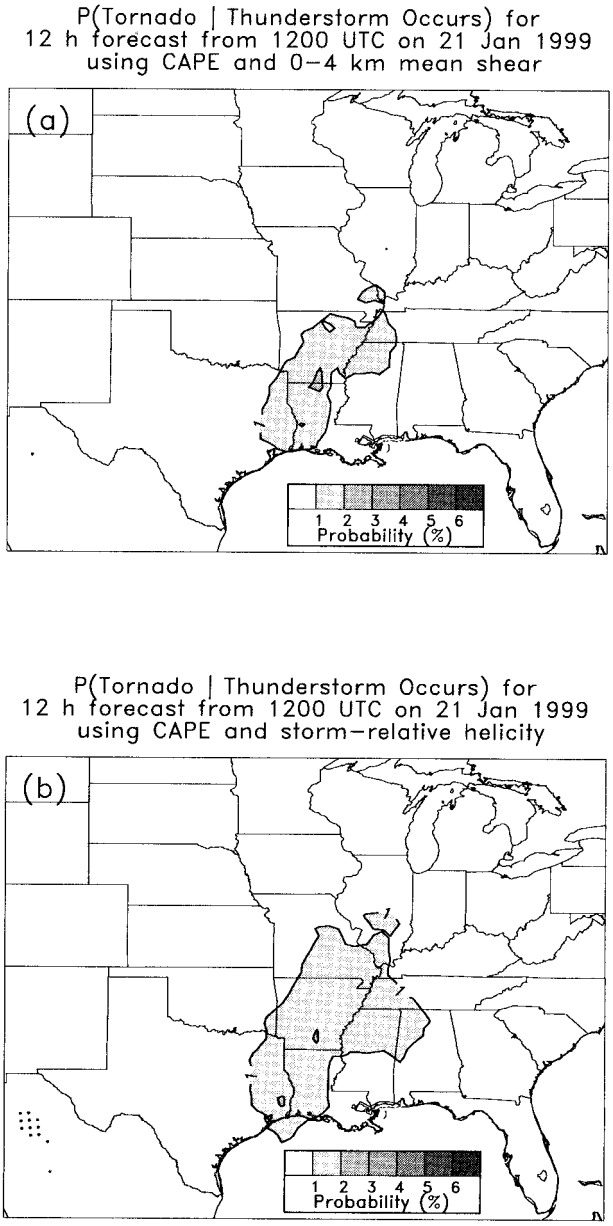

FIG. 14. Forecast conditional probabilities of the occurrence of a tornado given that a thunderstorm happens, for the forecast valid at 0000 UTC 22 Jan 1999. Compare to observations in Fig. 2. (a) Probabilities using CAPE and shear, and (b) using CAPE and helicity. Dotted areas indicate regions where probabilities should be regarded with suspicion because parameter values were outside the range of values used to develop the equations.

Because the model was developed using only 6 months of severe weather data, excluding any one case day with a major tornado outbreak can cause a substantial change in the probabilities, as will be demonstrated.

Tornado probability forecasts valid at 0000 UTC 22 January 1999 are shown in Figs. 14a,b. The model has a maximum of probability in northern Louisiana and overlapping the area of the tornado outbreak. These

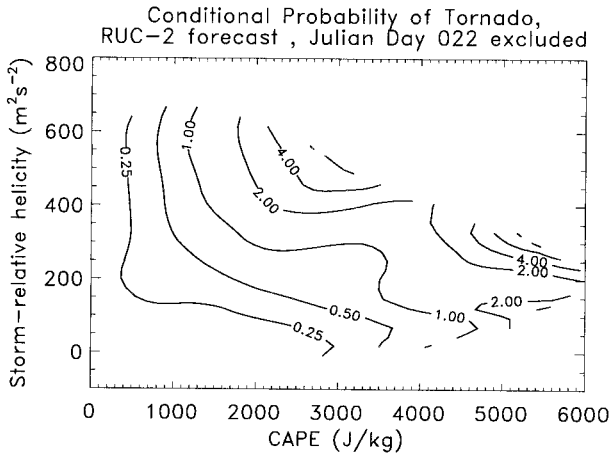

FIG. 15. As in Fig. 12b but excluding the observations in the 4-h period centered on 0000 UTC 22 Jan 1999.

probabilities would have been much higher had the cross-validation technique not been used and the 0000 UTC 22 January 1999 data not been included in the developmental data (Fig. 15). Comparing this figure against Fig. 12b, note that the probabilities at moderate CAPE and shear are dramatically lower when this case day is excluded. Hence, the longer the developmental period, the more reliable the tornado probabilities should be.

The forecasts for the Oklahoma City tornado outbreak at 0000 UTC 4 May 1999 are shown in Figs. 16a,b. The tornado probability maximum was forecast in south-central Texas, but there was also a relative maxima through Oklahoma and Kansas, overlapping the area struck by tornadoes. There was some convection associated with very large CAPE values in south-central Texas that day (Fig. 13).

Much of the region with high probabilities did not have convection, however. Since the maps display conditional probabilities *given that a thunderstorm occurs*, this does not necessarily indicate a problem with the model. It does highlight the need for additional guidance on the likelihood of thunderstorms of any type occurring. However, forecasting convective initiation is a tremendously complex problem, and a model for thunderstorm likelihood probably would require other information, such as the strength of low-level convergence and the amount of convective inhibition. We have some evidence that RUC-2 forecast convective inhibition may be useful as an additional predictor of thunderstorm likelihood. Using data points from Fig. 5, we examined the distribution of convective inhibition for data points where CAPE was greater that 2000 J kg^{-1} (Fig. 17). Distributions were plotted for both no thunderstorms and a composite of the three thunderstorm categories. Note that all other things being equal, the likelihood of convection occurring at high CAPE is reduced when there is a large amount of convective inhibition, as one might expect.

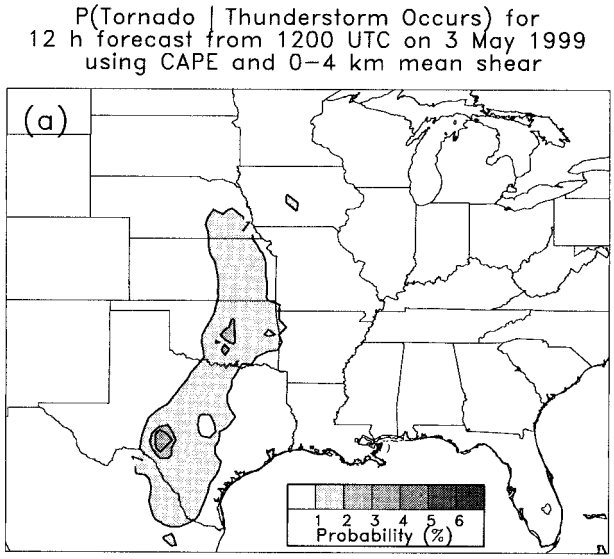

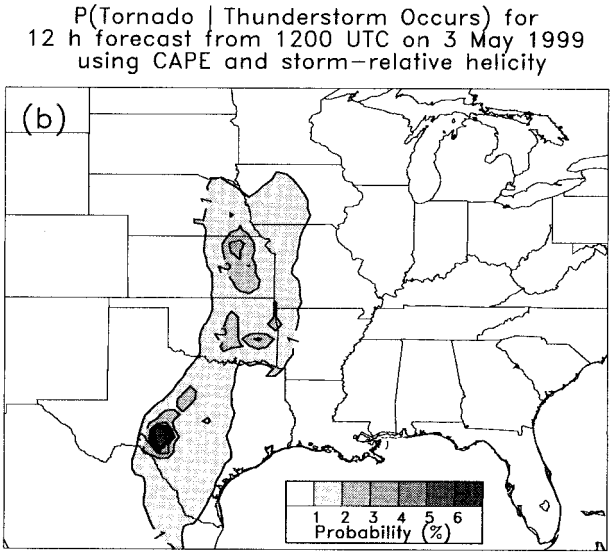

FIG. 16. As in Fig. 14 but for the date 0000 UTC 4 May 1999. Compare to gridded classification in Fig. 13.

6. Conclusions

This note described results from associating a classification of thunderstorm severity based on severe weather reports and lightning observations with RUC-2 analyses and forecasts. The purpose was both to compare and contrast these model-based results with the raob-based results such as in RB98 and to develop a probabilistic forecast model for conditional tornado likelihood. This model specifies the conditional probability that a significant tornado will occur given that a thunderstorm occurs and given that certain RUC-2

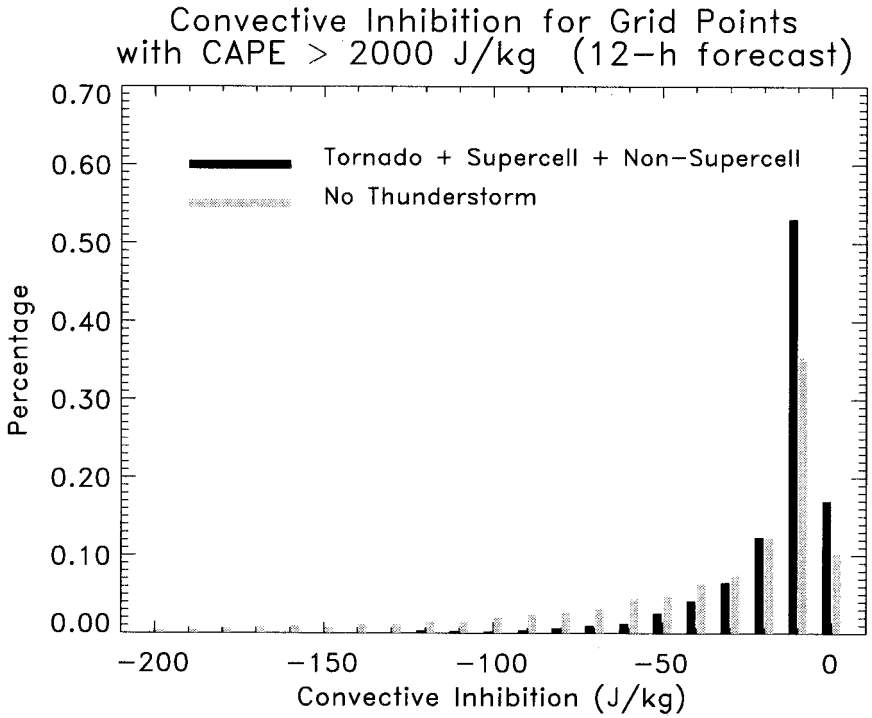

FIG. 17. Histogram of RUC-2 12-h forecast convective inhibition for subset of data points with CAPE > 2000 J kg^{-1}. Histograms are plotted for both a composite of the tornadic–supercellular–nonsupercellular categories and for the no thunderstorm category.

CAPE and shear (or CAPE and helicity) values are forecast.

RUC-2 analysis and forecast data provided a rather similar ability to distinguish between storm types as was observed by RB98 using raob data. This suggested such model data should be useful in a probabilistic forecast model of tornado likelihood.

Our probabilistic model was MOS-like in character but forecast conditional probabilities of significant tornadoes given a thunderstorm occurred. A few select cases demonstrated that the model does a reasonable job of predicting areas of enhanced risk for tornadoes. Like MOS, this model should perform best when the model physics are unchanged, and like MOS, it cannot correct for random model errors. Still, a probabilistic model like this one may be of use as a supplemental guidance tool for severe storms forecasters.

Many improvements to this prototype are envisioned once more data are available. First, a more robust classification methodology could be used, one that is tailored to the specific needs of severe weather forecasters. Ideally, the classification scheme and probabilistic models would be tailored to generate products to help forecasters with their sequential decision process: an improved model might thus forecast the likelihood of thunderstorms, the probability these thunderstorms will contain severe weather, and the conditional probability of various types of severe weather given that some severe weather occurs.

Beyond improving the classification and using more data, other changes may prove useful. For example, perhaps regional model biases in CAPE and shear can be corrected before a scheme such as this is applied. Also, it may be useful to develop forecasts for different lead times such as 3 or 6 h, for synoptic times other than 0000 UTC, and to use a wider variety of information in model development than just CAPE, shear, and helicity.

We hope to be able to do more extensive testing and development in the future in collaboration with operational forecasters.

Acknowledgments. The authors would like to thank Greg Thompson (NCAR/RAP) and Tracy Smith (NOAA/FSL) for their help in obtaining RUC-2 data. Tressa Kane and Randy Bullock (NCAR/RAP) provided assistance in obtaining and decoding the lightning network data. Mike Kay (NOAA/SPC) and Paul Polger (NWS/OM) kindly supplied the severe weather reports. Doug Nychka (NCAR/GSP) is thanked for his expertise in the development of nonparametric density estimates. Morris Weisman (NCAR/MMM) and Jeff Trapp (NOAA/NSSL) are thanked for substantive advice and for their informal reviews of this manuscript. Chuck

Doswell (NOAA/NSSL) and Steve Weiss (NOAA/SPC) are thanked for very thoughtful formal reviews.

REFERENCES

Benjamin, S. G., J. M. Brown, K. J. Brundage, B. Schwartz, T. Smirnova, T. L. Smith, L. L. Morone, and G. J. DiMego, 1998: The operational RUC-2. Preprints, *16th Conf. on Weather Analysis and Forecasting*, Phoenix, AZ, Amer. Meteor. Soc., 249–252.

Brooks, H. E., C. A. Doswell III, and R. A. Maddox, 1992: On the use of mesoscale and cloud-scale models in operational forecasting. *Wea. Forecasting*, **7,** 120–132.

——, ——, and J. Cooper, 1994a: On the environments of tornadic and nontornadic mesocyclones. *Wea. Forecasting*, **9,** 606–618.

——, ——, and R. B. Wilhelmson, 1994b: The role of midtropospheric winds in the evolution and maintenance of low-level mesocyclones. *Mon. Wea. Rev.*, **122,** 126–136.

Bunkers, H. J., B. A. Klimowski, J. W. Zeitler, R. L. Thompson, and M. L. Weisman, 2000: Predicting supercell motion using hodograph techniques. *Wea. Forecasting*, **15,** 61–79.

Carter, G. M., J. P. Dallavalle, and H. R. Glahn, 1989: Statistical forecasts based on the National Meteorological Center's numerical weather prediction system. *Wea. Forecasting*, **4,** 401–412.

Chisholm, A. J., and J. H. Renick, 1972: The kinematics of multicell and supercell Alberta hailstorms. Alberta Hail Studies, Research Council of Alberta Hail Studies Rep. 72-2, Edmonton, AB, Canada, 6 pp.

Davies, J. M., 1993: Hourly helicity, instability, and EHI in forecasting supercell tornadoes. Preprints, *17th Conf. on Severe Local Storms*, St. Louis, MO, Amer. Meteor. Soc., 107–111.

——, and R. H. Johns, 1993: Some wind and instability parameters associated with strong and violent tornadoes. 1. Wind shear and helicity. *The Tornado: Its Structure, Dynamics, Prediction, and Hazards*, *Geophys. Monogr.*, No. 79, Amer. Geophys. Union, 573–582.

Davies-Jones, R. P., 1984: Streamwise vorticity: The origin of updraft rotation in supercell storms. *J. Atmos. Sci.*, **41,** 2991–3006.

——, D. Burgess, and M. Foster, 1990: Test of helicity as a tornado forecast parameter. Preprints, *16th Conf. Severe Local Storms*, Kananaskis, AB, Canada, Amer. Meteor. Soc., 588–592

Doswell, C. A. III, S. J. Weiss, and R. H. Johns, 1993: Tornado forecasting—A review. *The Tornado: Its Structure, Dynamics, Prediction, and Hazards*, *Geophys. Monogr.*, No. 79, Amer. Geophys. Union, 557–572.

Droegemeier, K. K., S. M. Lazarus, and R. Davies-Jones, 1993: The influence of helicity on numerically simulated convective storms. *Mon. Wea. Rev.*, **121,** 2005–2029.

Fankhauser, J. C., and C. G. Mohr, 1977: Some correlations between various sounding parameters and hailstorm characteristics in northeast Colorado. Preprints, *10th Conf. on Severe Local Storms*, Omaha, NE, Amer. Meteor. Soc., 218–225.

Gilmore, M. S., and L. J. Wicker, 1998: The influence of midtropospheric dryness on supercell morphology and evolution. *Mon. Wea. Rev.*, **126,** 943–958.

Grice, G. K., and Coauthors, 1999: The golden anniversary celebration of the first tornado forecast. *Bull. Amer. Meteor. Soc.*, **80,** 1341–1348.

Hart, J. A., and W. Korotky, 1991: The SHARP workstation vl.50 users guide. National Weather Service, 30 pp. [Available from NWS Eastern Region Headquarters, 630 Johnson Ave., Bohemia, NY 11716.]

Islam, S., R. L. Bras, and K. A. Emanuel, 1993: Predictability of mesoscale rainfall in the tropics. *J. Appl. Meteor.*, **32,** 297–310.

Johns, R. H., and C. A., Doswell III, 1992: Severe local storms forecasting. *Wea. Forecasting*, **7,** 588–612.

——, J. M. Davies, and P. W. Leftwich, 1993: Some wind and instability parameters associated with strong and violent tornadoes. 2. Variations in the combination of wind and instability parameters. *The Tornado: Its Structure, Dynamics, Prediction, and Hazards*, *Geophys. Monogr.*, No. 79, Amer. Geophys. Union, 583–590.

Klemp, J. B., 1987: Dynamics of tornadic thunderstorms. *Annu. Rev. Fluid. Mech.*, **19,** 369–402.

——, and R. B. Wilhelmson, 1978: Simulations of right- and left-moving storms produced through storm splitting. *J. Atmos. Sci.*, **35,** 1097–1110.

Lilly, D. K., 1986: The structure, energetics and propagation of rotating convective storms. Part II: Helicity and storm stabilization. *J. Atmos. Sci.*, **43,** 126–140.

Lorenz, E. N., 1963: Deterministic non-periodic flow. *J. Atmos. Sci.*, **20,** 130–141.

——, 1969: The predictability of a flow which possesses many scales of motion. *Tellus*, **21,** 289–307.

Markowski, P. M., E. N. Rasmussen, and J. M. Straka, 1998a: The occurrence of tornadoes in supercells interacting with boundaries during VORTEX-95. *Wea. Forecasting*, **13,** 852–859.

——, J. M. Straka, E. N. Rasmussen, and D. O. Blanchard, 1998b: Variability of storm-relative helicity during VORTEX. *Mon. Wea. Rev.*, **126,** 2959–2971.

McCarthy, D., J. Schafer, and M. Kay, 1998: Watch verification at the Storm Prediction Center 1970–1997. Preprints, *19th Conf. on Severe Local Storms*, Minneapolis, MN, Amer. Meteor. Soc., 603–606.

Miller, R. C., 1972: Notes on the analysis and severe storms forecasting procedures of the Air Force Global Weather Central. Air Weather Service Tech Rep. 200 (rev.), 183 pp. [Available from Library, AFWA, Offutt AFB, NE 68113-5000; NTIS AD-744 042/XAB.]

Moncrieff, M. W., and M. J. Miller, 1976: The dynamics and simulation of tropical cumulonimbus and squall lines. *Quart. J. Roy. Meteor. Soc.*, **102,** 373–394.

Rasmussen, E. N., and D. O. Blanchard, 1998: A baseline climatology of sounding-derived supercell and tornado forecast parameters. *Wea. Forecasting*, **13,** 1148–1164.

——, S. Richardson, J. M. Straka, P. M. Markowski, and D. O. Blanchard, 2000: The association of significant tornadoes with a baroclinic boundary on 2 June 1995. *Mon. Wea. Rev.*, **128,** 174–191.

Reap, R. M., and D. S. Foster, 1979: Automated 12–36 hour probability forecasts of thunderstorms and severe local storms. *J. Appl. Meteor.*, **18,** 1304–1315.

Rogers, E., T. L. Black, D. G. Deaven, G. J. DiMego, Q. Zhao, M. Baldwin, N. W. Junker, and Y. Lin, 1996: Changes to the operational early eta analysis/forecast system at the National Centers for Environmental Prediction. *Wea. Forecasting*, **11,** 391–413.

Rotunno, R., and J. B. Klemp, 1982: The influence of the shear-induced pressure gradient on thunderstorm motion. *Mon. Wea. Rev.*, **110,** 136–151.

——, and ——, 1985: On the rotation and propagation of simulated supercell thunderstorms. *J. Atmos. Sci.*, **42,** 271–292.

Schlesinger, R. E., 1980: A three-dimensional numerical model of an isolated thunderstorm. Part II: Dynamics of updraft splitting and mesovortex couplet evolution. *J. Atmos. Sci.*, **37,** 395–420.

Silverman, B. W., 1986: *Density Estimation for Statistics and Data Analysis.* Chapman and Hall, 175 pp.

Smirnova, T. G., J. M. Brown, and S. G. Benjamin, 1997: Performance of different soil model configurations in simulating ground surface temperatures and surface fluxes. *Mon. Wea. Rev.*, **125,** 1870–1884.

Stensrud, D. J., J. V. Cortinas Jr., and H. E. Brooks, 1997: Discriminating between tornadic and nontornadic thunderstorms using mesoscale model output. *Wea. Forecasting*, **12,** 613–632.

Weisman, M. L., 1996: On the use of vertical wind shear vs. helicity in interpreting supercell dynamics. Preprints, *18th Conf. on Severe Local Storms*, San Francisco, CA, Amer. Meteor. Soc., 200–203.

——, and J. B. Klemp, 1982: The dependence of numerically simulated convective storms on vertical wind shear and buoyancy. *Mon. Wea. Rev.*, **110,** 504–520.

——, and ——, 1984: The structure and classification of numerically simulated convective systems in directionally varying wind shears. *Mon. Wea. Rev.,* **112,** 2479–2498.
——, and ——, 1986: Characteristics of isolated convective storms. *Mesoscale Meteorology and Forecasting,* P. S. Ray, Ed., Amer. Meteor. Soc., 331–358.
——, and R. Rotunno, 2000: On the use of vertical wind shear versus helicity in interpreting supercell dynamics. *J. Atmos. Sci.,* **57,** 1452–1472.
Wilks, D. S., 1995: *Statistical Methods in the Atmospheric Sciences: An Introduction.* Academic Press, 467 pp.
Yucel, I., J. W. Shuttleworth, J. Washborne, and F. Chen, 1998: Evaluating NCEP Eta Model–derived data against observations. *Mon. Wea. Rev.,* **126,** 1977–1991.